UC Irvine
UC Irvine Previously Published Works

Title

Charybdotoxin Binding in the IKs Pore Demonstrates Two MinK Subunits in Each Channel Complex

Permalink

https://escholarship.org/uc/item/0zb0n82w

Journal

Neuron, 40(1)

ISSN

0896-6273

Authors

Chen, Haijun
Kim, Leo A
Rajan, Sindhu
et al.

Publication Date

2003-09-01

DOI

10.1016/s0896-6273(03)00570-1

Copyright Information

Peer reviewed

Charybdotoxin Binding in the I_{Ks} Pore Demonstrates Two MinK Subunits in Each Channel Complex

Report

Haijun Chen,[1] Leo A. Kim,[1]
Sindhu Rajan, Shuhua Xu,
and Steve A.N. Goldstein*
Department of Pediatrics
Department of Cellular and Molecular Physiology
Boyer Center for Molecular Medicine
Yale University School of Medicine
295 Congress Avenue
New Haven, Connecticut 06536

Summary

I_{Ks} voltage-gated K$^+$ channels contain four pore-forming KCNQ1 subunits and MinK accessory subunits in a number that has been controversial. Here, I_{Ks} channels assembled naturally by monomer subunits are compared to those with linked subunits that force defined stoichiometries. Two strategies that exploit charybdotoxin (CTX)-sensitive subunit variants are applied. First, CTX on rate, off rate, and equilibrium affinity are found to be the same for channels of monomers and those with a fixed 2:4 MinK:KCNQ1 valence. Second, ^{3}H-CTX and an antibody are used to directly quantify channels and MinK subunits, respectively, showing 1.97 ± 0.07 MinK per I_{Ks} channel. Additional MinK subunits do not enter channels of monomeric subunits or those with fixed 2:4 valence. We conclude that two MinK subunits are necessary, sufficient, and the norm in I_{Ks} channels. This stoichiometry is expected for other K$^+$ channels that contain MinK or MinK-related peptides (MiRPs).

Introduction

Voltage-gated K$^+$ channels in native cells are mixed assemblies of four pore-forming α subunits and accessory β subunits that dictate cell-specific operation. *KCNE*-encoded MinK-related peptides (MiRPs) are single-span transmembrane β subunits whose control of surface expression, gating kinetics, ion conduction, and pharmacology is emerging in an increasing number of channels (Abbott and Goldstein, 1998, 2002). I_{Ks} channels in heart and ear are formed by KCNQ1 (KvLQT1) and MinK subunits (Barhanin et al., 1996; Sanguinetti et al., 1996). Inherited missense mutations in both subunits are associated with cardiac arrhythmia and deafness (Schulze-Bahr et al., 1997; Splawski et al., 1997; Sesti and Goldstein, 1998). The number of MinK subunits in I_{Ks} channels has been uncertain. We argued for two MinK subunits per channel based on suppression of current when wild-type MinK was expressed with a MinK mutant (Wang and Goldstein, 1995). Others studied mixtures with different MinK variants and concluded I_{Ks} channels have variable stoichiometry with four or more MinK subunits (Tzounopoulos et al., 1995; Wang et al., 1998).

Here, we reassess MinK valence in I_{Ks} channels by two new strategies, one biophysical, and the other biochemical. In both approaches, we exploit a KCNQ1 mutant (Kv*) engineered to be highly sensitive to charybdotoxin (CTX) (K_i ~1 nM). CTX is a useful probe of K$^+$ channels because it binds with one-to-one stoichiometry to occlude the ion conduction pore (Miller et al., 1985; MacKinnon and Miller, 1988; Goldstein and Miller, 1993). The opportunity to reevaluate MinK valence was suggested when CTX affinity was found to vary ~140-fold if I_{Ks} channels were formed with Kv* and wild-type MinK (M) or a MinK variant (HM). First, CTX block of channels assembled naturally of HM and Kv* subunits, and those with fixed stoichiometries due to subunit linkage were compared; inhibition kinetics and equilibrium affinity for natural I_{Ks} channels were found to match channels forced to carry two HM (formed by two HM-Kv*-Kv* subunits) but not those with four HM (composed of four HM-Kv* subunits). Judged by block kinetics, two HM appeared to be the normal number, as only a single channel type was apparent despite 10-fold variation in the HM to Kv* cRNA ratio, expression of HM-Kv*-Kv* alone, or HM-Kv*-Kv* with excess M or HM subunits.

In a second approach, I_{Ks} channel stoichiometry was directly assessed by two binding assays performed in parallel. To measure surface channel number, radiolabeled recombinant CTX was applied to cells expressing channels formed by HM + Kv* or HM-Kv*-Kv* or HM-Kv* subunits. Concurrently, a monoclonal antibody was used to quantify surface HM subunits on matched samples by luminometry. Thereby, an HM to channel ratio (ν) was determined and showed naturally assembled HM + Kv* channels to contain two HM subunits: half those in HM-Kv* channels and the same number as in HM-Kv*-Kv* channels.

Results

Kv*, a CTX-Sensitive KCNQ1 Mutant

Identification of α subunit residues important for high-affinity toxin binding in Shaker and Kv1.3 K$^+$ channels pointed to the pore-forming (P loop) residues (MacKinnon and Miller, 1989), allowed indirect mapping of the outer pore based on the structure of CTX (Goldstein et al., 1994; Ranganathan et al., 1996), and directed rational mutation of toxin-insensitive channels, such as Kv2.1, to yield CTX blockade (Goldstein and Miller, 1992; Gross et al., 1994). Based on these findings and homology among the P loop regions of KCNQ1, Kv1.3, and Kv2.1, a functional, CTX-sensitive KCNQ1 variant (Kv*) was produced through an iterative process that resulted in 5 point mutations and deletion of a 4 residue stretch (Figure 1A). Whereas 10 nM CTX had no effect on wild-type KCNQ1 channels expressed in oocytes and studied by two-electrode voltage clamp, it blocked ~80% of current through Kv* channels (Figure 1B, arrows). Similarly, I_{Ks} channels formed with wild-type MinK (M) and KCNQ1 were insensitive to 10 nM CTX while M + Kv* channels were suppressed ~45% (Figure 1C).

*Correspondence: steve.goldstein@yale.edu
[1] These authors contributed equally to this work.

A


```
S5              Pore loop                    S6
DAVNESGRVEFGSYADALWWGVVTVTTIGYGDKVPQTWVGK    KCNQ1
DDPTS----GFSSIPDAFWWAVVTMTTVGYGDMHPVTIGGK    Kv1.3
DEDDT----KFKSIPASFWWATITMTTVGYGDIYPKTLLGK    Kv2.1
DAVNS----GFGSYADALWWGVVTVTTIGYGDIYPVTWVGK    Kv*
     * * * * * *                   ** *
```
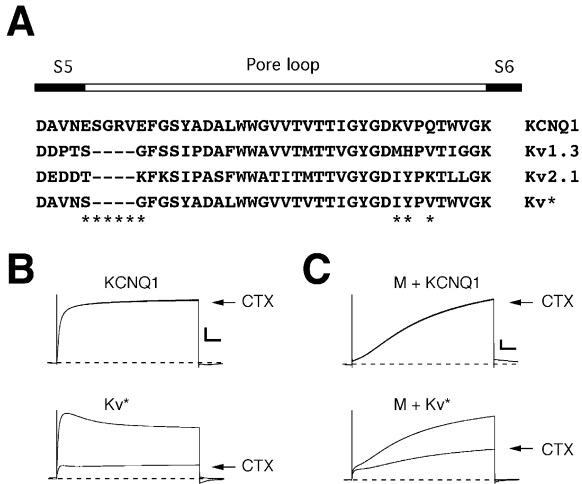
B

C

Figure 1. Charybdotoxin-Sensitive KCNQ1 Variant and I_{Ks} Channels

(A) Pore loop region sequences of wild-type human KCNQ1 (residues 286–326 shown), rat Kv1.3, rat Kv2.1, and a charybdotoxin (CTX)-sensitive KCNQ1 variant (Kv*) mutant. Dashes represent gaps. The mutated residues in Kv* channels are noted (asterisk). KCNQ1 (P51787); rat Kv1.3 (P15384); rat Kv2.1 (P15387); and Kv* (AY320286).
(B) KCNQ1 channels are insensitive to CTX, whereas Kv* channels are blocked. Raw whole-oocyte currents before and after (←) application of 10 nM CTX. Recording protocol: cells at −90 mV, stepped to a test voltage of 20 mV for 5 s every 10 s; CTX added after 4 stable cycles; pulses 5 and 30 shown. Scale bars equal 0.5 s, 0.5 μA.
(C) M + KCNQ1 channels are insensitive to CTX, whereas M + Kv* channels are blocked. Whole-oocyte currents before and after (←) application of 10 nM CTX. Protocol and scale bar are as in (B).

Channels formed with Kv* operated much like those with wild-type KCNQ1 subunits despite these draconian modifications. Kv* channels did show partial inactivation on depolarization above 20 mV (Figure 1B), a known effect of KCNQ1 P loop mutations (Seebohm et al., 2001); however, the mutations did not alter half-maximal activation voltage ($V_{0.5}$), slope factor (V_s), or selectivity for K$^+$ over sodium as judged by shift in whole-cell reversal potential (ΔE_{rev}) on changing bath K$^+$ from 2 to 20 mM by replacement for sodium ($V_{0.5}$ = −31.3 ± 0.6 mV; V_s = −14.6 ± 1.8 mV; ΔE_{rev} = 48.4 ± 1.4 mV; n = 5–6 compared to KCNQ1 channels with $V_{0.5}$ = −28.9 ± 1.2 mV; V_s = −17.6 ± 1.7 mV; ΔE_{rev} = 50.4 ± 1.3 mV; n = 6). Moreover, Kv* subunits assembled with M to produce I_{Ks} channels that were indistinguishable from those with KCNQ1—so long as they were not exposed to CTX (Figure 1C). Thus, M + Kv* and M + KCNQ1 I_{Ks} channels were found to be alike ($V_{0.5}$ = ~27.0 ± 2.2 mV; V_s = −18.3 ± 1.2 mV; ΔE_{rev} = 50.9 ± 2.5 mV; n = 5–6; and $V_{0.5}$ = ~23.5 ± 2.3 mV; V_s = −19.6 ± 1.3 mV; ΔE_{rev} = 47.4 ± 2.4 mV; n = 6–9; respectively), assessed via isochronal studies because I_{Ks} currents do not saturate (Wang and Goldstein, 1995; Sesti and Goldstein, 1998).

MinK Subunits Alter CTX Block of I_{Ks} Channels

As suggested by trials with 10 nM CTX (Figure 1), dose-response studies confirmed that MinK subunits altered the high-affinity CTX site in Kv*. Whereas application of 200 nM CTX did not suppress wild-type KCNQ1 channels, half-maximal blockade at equilibrium (K_i) for Kv* channels was achieved at 0.93 ± 0.11 nM CTX (Figure
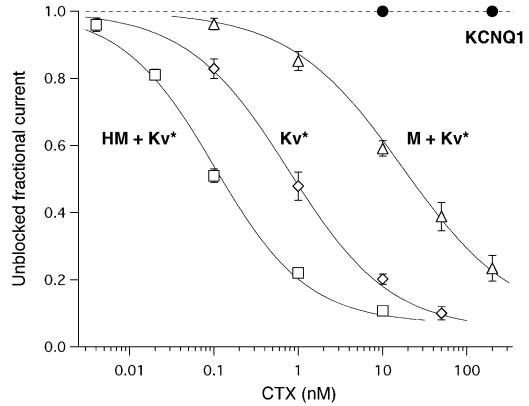

Figure 2. MinK and HM Alter CTX Block of I_{Ks} Channels Formed with Kv* Subunits

CTX block of channels formed by Kv* or M + Kv* or HM + Kv* subunits by protocol in Figure 1B; continuous lines are fits to Equation 7 and yield K_i = 0.93 ± 0.11 nM, 0.11 ± 0.02 nM, and 15.7 ± 2.1 nM, with h of 0.78, 0.82, and 0.72, respectively. KCNQ1 channels showed no inhibition at 200 nM CTX. Each data point is mean ± SEM for 6–23 oocytes.

2). On incorporation of MinK, CTX affinity decreased ~17-fold (K_i = 15.7 ± 2.1 nM for M + Kv* channels). Conversely, a MinK variant (HM) with a modified external domain including a 9 residue hemagluttinin epitope was found to enhance CTX blockade; HM + Kv* channels (characterized by $V_{0.5}$ = −1.1 ± 1.1 mV; V_s = −18.9 ± 0.9 mV; ΔE_{rev} = 50.0 ± 1.2 mV; n = 6–9) had a K_i of 0.11 ± 0.02 nM, which is ~9-fold more sensitive than Kv* channels and ~140-fold more sensitive than M + Kv* channels.

$$\text{Channel} + \text{CTX} \underset{K_{off}}{\overset{K_{on}}{\rightleftarrows}} \text{Channel:CTX} \qquad (1)$$
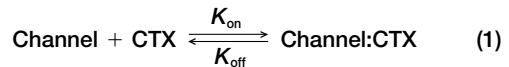
As one CTX molecule blocks one channel pore (Equation 1), the time course for relaxation to equilibrium inhibition on abrupt exposure to toxin depends on toxin concentration (a second-order association process), while dissociation (unblock) is first order and a direct reflection of stability of toxin on its pore site when toxin is removed abruptly and completely (Miller et al., 1985; MacKinnon and Miller, 1988; Goldstein and Miller, 1993). Consistent with high-affinity CTX binding, unblock of Kv* channels was not complete even after 25 min (Figure 3A). Calculated K_i and concentration-independent association and dissociation rate constants for channels studied in this report are determined according to Equations 3–7 (see Experimental Procedures) and collected in Table 1. These assessments revealed M had little effect on toxin on rate compared to channels with Kv* alone (K_{on} = 1.9 ± 0.3 μM^{-1}s^{-1} versus 1.5 ± 0.2 μM^{-1}s^{-1}, respectively) but destabilized bound CTX to speed its off rate over 20-fold (K_{off} = 30.8 ± 3.9 × 10^{-3} s^{-1} versus 1.4 ± 0.3 × 10^{-3} s^{-1}, respectively) (Figure 3B). Conversely, HM increased inhibition not by stabilizing bound toxin but by enhancing the concentration-independent association rate constant ~35-fold (K_{on} = 51.8 ± 5.2 μM^{-1}s^{-1}) while increasing dissociation kinetics ~3-fold (K_{off} = 5.0 ± 0.6 × 10^{-3} s^{-1}) (Figure 3C).
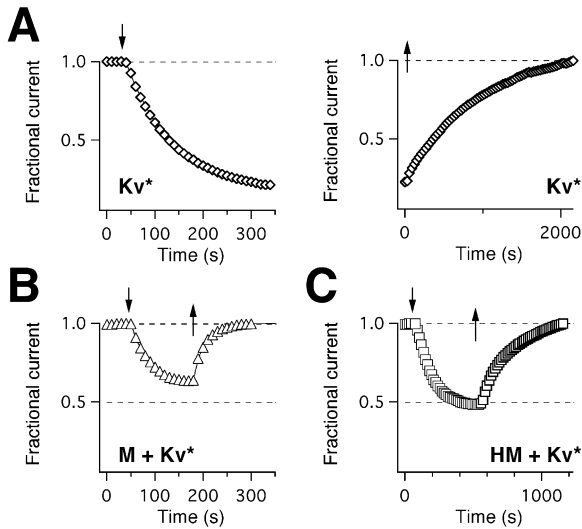
Figure 3. CTX Block Kinetics: Channels Assembled of Monomers

Block and unblock time course with abrupt CTX addition (↓) and removal (↑) by exchange of the bath solution. Inhibition was fit to a single exponential function: $I_∞ + I_α*e^{(-t/\tau)}$, where $I_∞$ and $I_α$ are constants; values in Table 1. For block, τ represents τ_{on} in Equation 3 and $I_∞$ is f_u in Equation 5; for unblock, τ represents τ_{off} in Equation 4, $I_∞ = 1$, and $I_α$ is f_u in Equation 5. Protocol as in Figure 1B.

(A) Block (left panel) of Kv* channels by 10 nM CTX expressed in an oocyte; unblock (right panel) of same cell. For this sample cell, $\tau_{on} = 96.6$ s and $\tau_{off} = 951.2$ s.

(B) Block and unblock kinetics of M + Kv* channels by 10 nM CTX. For this cell, $\tau_{on} = 40.1$ s and $\tau_{off} = 24.5$ s.

(C) Block and unblock kinetics of HM + Kv* channels by 0.1 nM CTX. For this cell, $\tau_{on} = 122.1$ s and $\tau_{off} = 231.7$ s.

CTX Block Reflects Two HM Subunits in Naturally Assembled I_{ks} Channels

We sought to exploit the effects of HM on CTX block kinetics to assess the composition of I_{ks} channels. Prior work by others had shown MinK-KCNQ1-KCNQ1 and MinK-KCNQ1 subunits could successfully form channels that functioned not unlike natural I_{ks} (Wang et al., 1998). First, we compared channels assembled of HM + Kv* monomers and those with HM-Kv*-Kv* subunits (where dimeric assembly gives a 2:4 HM:Kv* subunit ratio) or HM-Kv* subunits (where tetrameric assembly yields a 4:4 ratio). As expected, both HM-Kv*-Kv* and HM-Kv* channels produced slowly activating, K⁺-selective, I_{ks}-like channels ($V_{0.5} = -5.1 ± 1.0$ mV; $V_s = -18.6 ± 0.6$ mV; $\Delta E_{rev} = 48.8 ± 1.3$ mV; and $V_{0.5} = -4.5 ± 1.7$ mV; $V_s = -19.7 ± 0.7$ mV; $\Delta E_{rev} = 51.3 ± 1.9$ mV, respectively, n = 5–6) (Figure 4A). The channels varied, however, in their response to 0.1 nM CTX. Toxin association (Figure 4B) and dissociation kinetics (Figure 4C) for HM + Kv* channels were like those for HM-Kv*-Kv* channels but different from HM-Kv* channels (Table 1). Both CTX block and unblock with HM-Kv* channels were ~2-fold faster than for HM-Kv*-Kv* channels (equilibrium affinity was little changed as kinetics effects were off-setting). The results argue for equivalence of I_{ks} channels formed by HM + Kv* or HM-Kv*-Kv* subunits and, therefore, inclusion of two HM subunits into each channel of either type.

Binding Assays Indicate Two HM Subunits in Naturally Assembled I_{ks} Channels

Radioactive CTX has previously been used to estimate the number of Shaker K⁺ channels on the surface of COS cells (Sun et al., 1994) and on oocytes to calculate
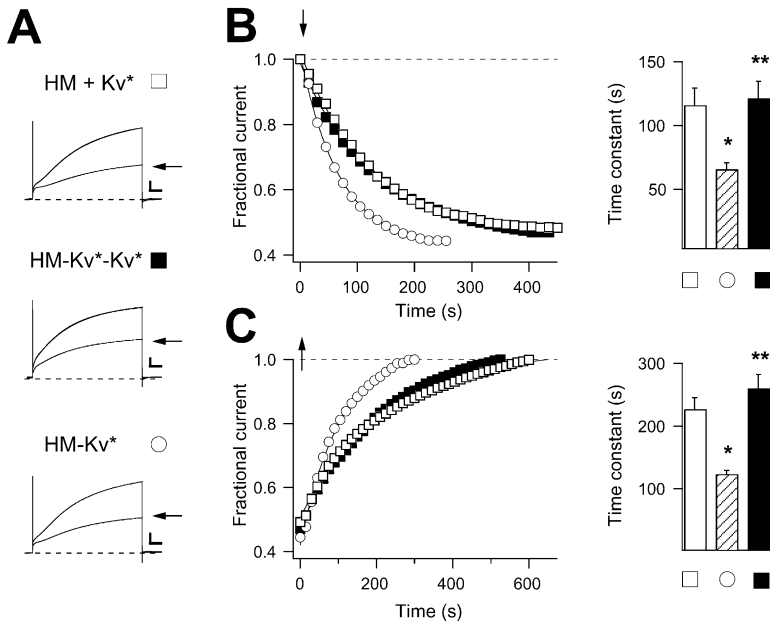
Table 1. CTX Blocking Parameters for Various Channel Complexes

Channels	Calculated K_i	K_{on}	K_{off}	Number of Oocytes
	(nM)	($\mu M^{-1}s^{-1}$)	($s^{-1} × 10^{-3}$)	
Monomers				
Kv*	1.1 ± 0.3	1.5 ± 0.2	1.4 ± 0.3	14
M + Kv*	14.1 ± 1.2	1.9 ± 0.3	30.8 ± 3.9	15
HM + Kv* (1)[a]	0.09 ± 0.01	52.0 ± 3.5	4.6 ± 0.5	19
Linked subunits				
HM-Kv*	0.13 ± 0.01	95.5 ± 8.4	8.8 ± 0.4	48
HM-Kv*-Kv*	0.11 ± 0.01	51.0 ± 5.8	4.3 ± 0.4	24
Controls				
HM + Kv* (0.2)[a]	0.11 ± 0.01	51.8 ± 5.2	5.0 ± 0.6	22
HM + Kv* (2)[a]	0.09 ± 0.01	60.1 ± 4.7	4.8 ± 0.3	21
Kv*-Kv*	1.0 ± 0.2	1.7 ± 0.2	1.6 ± 0.2	4
HM + Kv*-Kv*	0.10 ± 0.02	53.8 ± 8.8	4.4 ± 1.0	4
HM + HM-Kv*-Kv*	0.11 ± 0.01	59.7 ± 12.1	5.2 ± 0.6	11
M + HM-Kv*-Kv*	0.18 ± 0.01	41.5 ± 4.7	5.6 ± 0.8	12
HM-Kv*-KCNQ1	9.2 ± 0.8	2.7 ± 0.2	23.8 ± 0.8	7
HM-KCNQ1-Kv*	12.3 ± 0.7	2.3 ± 0.2	27.6 ± 2.0	13
M-Kv*	16.4 ± 0.8	1.6 ± 0.1	25.1 ± 1.0	39
M-Kv*-Kv*	14.4 ± 0.9	2.2 ± 0.2	27.9 ± 1.8	15
HM + M-Kv*-Kv*	12.0 ± 1.2	1.9 ± 0.2	30.5 ± 2.6	17

CTX blocking parameters and K_i here calculated according to Equations 1 and 3–7 using CTX at level near K_i; in legends to Figures 2 and 4, indicated K_i differs slightly from this table as they were from fits to dose response.
Abbreviations: M, MinK; HM, MinK variant; Kv*, the CTX-sensitive KCNQ1 mutant; +, co-expression.
[a] Numbers in parentheses indicate injected cRNA ratio HM to Kv*.

Figure 4. CTX Block Kinetics: HM + Kv* and HM-Kv*-Kv* Channels Are Alike

CTX block and unblock for HM-Kv* and HM-Kv*-Kv* channels by protocol in Figure 1B, fit as in Figure 2 to Equation 7, yields $K_i = 0.10 \pm 0.03$, 0.11 ± 0.03 nM with h of 0.80 and 0.76, respectively, n = 15–41 (not shown). Statistical significance determined by two-tailed t test; *, different, $p < 0.01$; **, not different, $p > 0.05$).

(A) Whole-oocyte currents for cells expressing HM + Kv*, HM-Kv*-Kv*, or HM-Kv* channels before and after (←) application of 0.1 nM CTX. Scale bars equal 0.5 s, 0.5 μA.

(B) Block kinetics with 0.1 nM CTX for HM + Kv*, HM-Kv*-Kv*, or HM-Kv* channels (left panel) shows overlap of the time course for inhibition of HM + Kv* (open square) and HM-Kv*-Kv* (filled square) channels but not HM-Kv* (circle). Continuous lines are fits as in Figure 3. Right panel is mean $\pm$ SEM for $\tau_{on} = 116.0 \pm 13.5$, n = 15; 122 ± 13.2, n = 16; and 65.6 ± 5.2, n = 41; for HM + Kv*, HM-Kv*-Kv*, and HM-Kv*, respectively.

(C) Unblock kinetics for oocytes in (B, left panel) shows overlap of the time course for inhibition of HM + Kv* (open square) and HM-Kv*-Kv* (filled square) but not HM-Kv* (circle). Continuous lines are fits as in Figure 3. Right panel is mean $\pm$ SEM for $\tau_{off} = 227 \pm 18.4$, n = 15; 260 ± 22.5, n = 16; and 124 ± 6.1, n = 41; for HM + Kv*, HM-Kv*-Kv*, and HM-Kv*, respectively.

the gating charge movement of single channels (Aggarwal and MacKinnon, 1996). So, too, monoclonal antibodies and enzyme amplification have been used to quantify surface expression of ion channel subunits on oocytes (Zerangue et al., 1999; O'Kelly et al., 2002) and yeast cell spheroplasts (Sesti et al., 2003). We combined these two assays to assess subunit stoichiometry using ³H-CTX to count channels and antibody binding with luminometry to assess HM subunit levels on paired samples (in duplicate or triplicate) in three independent trials.

Naturally assembled HM + Kv* channels were compared to HM-Kv*-Kv* and HM-Kv* channels using COS7 mammalian tissue culture cells. As CTX binds to all three channel types with high affinity ($K_i \approx 0.1$ nM) and toxin dissociation during rapid wash steps was the same (Experimental Procedures), it was possible to estimate the number of channels on groups of cells by incubation with excess ³H-CTX (34 nM) and measurement of specifically bound radioactive toxin using the specific activity of the preparation and the knowledge that toxin:channel interaction is 1:1 (Figure 5A, top). The number of HM + Kv* channels per COS7 cell from ³H-CTX binding was $8.4 \pm 3.2 \times 10^5$ (n = 3 trials). Rat monoclonal antibodies to HA applied to matching groups of cells bound specifically to surface HM subunits and were quantified with a peroxidase-conjugated secondary antibody and chemiluminescence (Figure 5A, bottom). As signals from both assays increased in linear fashion with binding site number (Sun et al., 1994; Aggarwal and MacKinnon, 1996; Zerangue et al., 1999; O'Kelly et al., 2002; Sesti et al., 2003), it followed that specific radioactive counts correlated directly with channel number (Figure 5B, CPM), specific light units corresponded to HM number (Figure 5B, RLU), and the ratio of the light and radioactive signals offered a parameter directly proportional to the number of HM subunits per channel, v (Equation 2). If subunits linked in tandem fold and assemble according to the dictates of their primary sequences, v for cells expressing HM-Kv*-Kv* subunits should be half that for cells expressing HM-Kv* subunits. This was found to be the case in three trials (Figure 5C). Moreover, v for channels formed by assembly of HM + Kv* or HM-Kv*-Kv* were indistinguishable (Figure 5C). If channels formed by HM-Kv*-Kv* have two HM subunits per channel, those formed by HM-Kv* contain 4.23 ± 0.27 HM subunits, and those with HM + Kv* carry 1.97 ± 0.07 HM subunits.

$$v = \text{specific light units (HM subunits)/}$$

$$\text{specific } {}^3\text{H-CTX (channels)} \qquad (2)$$

An estimate of two HM subunits in each channel could be too low if many Kv* channels (without HM) are present on cells expressing HM + Kv*. This did not appear to be the case; first, fewer than 5% of cells showed rapidly activating K^+ current consistent with the formation of Kv* channels when cells expressing both subunits were studied by patch-clamp. Second, whole-cell I_{Ks} currents were ~15-fold greater for oocytes expressing HM + Kv* compared to those with only Kv* (not shown), a canonical effect of MinK on KCNQ1 (Sanguinetti et al., 1996) that can be explained only in part by a 3- to 4-fold increase in unitary conductance (Sesti and Goldstein, 1998). The estimate of two HM subunits per channel could be too high if surplus HM subunits (without Kv*) reached the cell surface. This also did not appear to be confounding as cells expressing only HM subunits had light signals ~3-fold smaller than those with both HM and Kv* subunits (n = 2).

The Fitness of Channels Formed with Linked Subunits

The conclusion from CTX blocking and binding studies that naturally assembled I_{Ks} channels contain two HM subunits was based on similar results with HM + Kv* and HM-Kv*-Kv* channels. It was therefore important
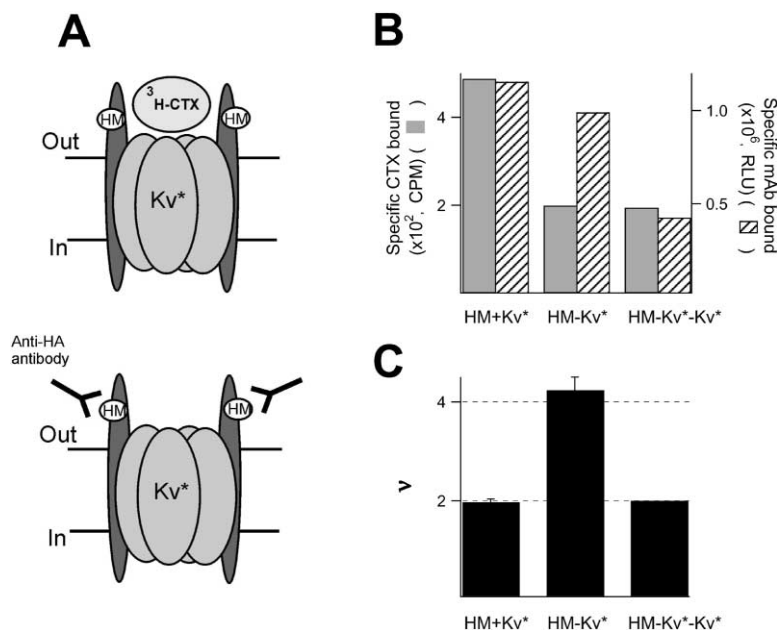
Figure 5. Binding Assays for HM Subunits and I_{Ks} Channels

(A) Cartoon depicts methods: CTX binding to assess channel number (top) and anti-HA monoclonal antibody binding (bottom) to HM subunits on surface of COS7 cells.

(B) Raw signals from one assay. [³H]-NEM-CTX binding and chemiluminescent (RLU) signals. These groups of cells expressed 46.8×10^9 HM + Kv* channels, 18.6×10^9 HM-Kv*-Kv* channels, and 19.1×10^9 HM-Kv* channels.

(C) The relative number of HM subunits in HM + Kv* and HM-Kv* channels based on three assays as in (B) as calculated by Equation 2, setting ν for HM-Kv*-Kv* as 2 gave 1.97 ± 0.07 and 4.23 ± 0.27, respectively.

to confirm that all three subunits linked in HM-Kv*-Kv* subunits gained representation in the channels. In support of contribution by HM, HM-Kv*-Kv* channels activated slowly and showed enhanced CTX affinity compared to Kv* alone (Table 1). To test that both the first and second Kv* subunits contributed to pore formation in HM-Kv*-Kv* channels, two additional linked subunits, HM-KCNQ1-Kv* and HM-Kv*-KCNQ1, were created and studied with CTX and the smaller pore-blocker, tetra-ethylammonium ion (TEA). CTX block supported the presence of both wild-type and mutant pore-forming subunits in the channels because equilibrium affinity was diminished and block kinetics altered by inclusion of wild-type KCNQ1 in either the first or second position (Table 1).

Study of TEA block offered crisp additional support for contribution of both pore-forming subunits in linked subunits to the pore. While wild-type KCNQ1 channels were insensitive to TEA ($K_i > 100$ mM), Kv* and HM + Kv* channels had equilibrium blocking constants of 0.53 ± 0.05 mM and 0.55 ± 0.05 mM, respectively (20 mV, n = 6 oocytes). This was expected, as a KCNQ1 mutant with just two of the changes in Kv* (K318I, V319Y) showed enhanced TEA sensitivity that was unaltered by MinK (Kurokawa et al., 2001). The affinity of TEA for HM-Kv*-Kv* channels was like that for naturally formed HM + Kv* channels, $K_i = 0.52 \pm 0.03$ mM (n = 6). In contrast, HM-KCNQ1-Kv* and HM-Kv*-KCNQ1 channels had reduced TEA sensitivity, showing $K_i = 17.2 \pm 0.9$ mM and 16.9 ± 1.1 mM, respectively (n = 6–10). This recapitulated the shift in affinity observed when Kv1.1 channels formed with four TEA-sensitive subunits were compared to channels with two sensitive and two insensitive subunits, from $K_i \sim 0.5$ to 18 mM TEA, $\Delta\Delta G \sim 8.8$ Kj/mol (Kavanaugh et al., 1992).

One Natural Subunit Valence for I_{Ks} Channels

While an estimate of two HM subunits in each I_{Ks} channel could be an average if HM + Kv* subunits assemble with multiple stoichiometries, we failed to obtain evidence for

more than one type of I_{Ks} channel in sensitive studies of CTX block. Despite altering the ratio of HM:Kv* cRNA injected into oocytes over a 10-fold range to encourage alternate stoichiometries, no significant changes in toxin association or dissociation rate were observed (Table 1) and no rapidly activating currents emerged (to suggest formation of Kv* channels). Further, channels of HM-Kv*-Kv* (or M-Kv*-Kv*) subunits appeared to be "complete" and to exclude additional subunits as they were blocked like naturally assembled channels even when coexpressed with HM or M subunits (Table 1). So, HM assembled with Kv*-Kv* to yield channels blocked by CTX like channels of HM + Kv* or HM-Kv*-Kv* but did not alter block of HM-Kv*-Kv* channels (based on HM-Kv* channel behavior, extra incorporated HM should increase toxin on rate). Similarly, HM-Kv*-Kv* channels were insensitive to coexpressed M (despite the ~140-fold difference in CTX affinity for Kv* channels with M rather than HM). Moreover, M-Kv*-Kv* channels showed no increase in CTX block on expression with HM as expected if the subunit had been incorporated. These findings support the conclusion that I_{Ks} channels form with one natural valence: two MinK and four KCNQ1 subunits.

Discussion

The number of MinK monomers in each I_{Ks} channel has been a subject of controversy. Here, two new strategies were applied to address the problem: one indirect (examining the kinetics of pore blockade by CTX) and another direct (assessing binding of radioactive CTX [to count channels] and a monoclonal antibody [to quantify MinK subunits]). Both methods employed a CTX-sensitive variant of KCNQ1 (Kv*) and a modified MinK (HM) and compared channels naturally assembled of monomer subunits and those with linked subunits that forced formation of channels with defined subunit stoichiometry. First, I_{Ks} channels assembled of HM + Kv* subunits were observed to have the same functional attributes

and CTX block parameters as those with HM-Kv*-Kv* subunits but to differ from those with HM-Kv* subunits. Second, binding studies indicated that 1.97 ± 0.07 HM subunits and 4 Kv* subunits were in each channel complex assembled of monomers. Neither varying the ratio of expressed monomer subunits nor adding free M or HM subunits during channel biosynthesis with "complete" linked subunits (i.e., HM-Kv*-Kv*) increased apparent MinK valence, as judged by blockade. These results argued that each I_{Ks} channel contained two MinK and four KCNQ1 subunits and that alternative subunit numbers were not naturally assembled.

The strength of these conclusions depends on three factors: first, the integrity of CTX as a probe of K+ channel pore structure. CTX was chosen for this study precisely because it is suited to the task. The toxin binds with high affinity only when four permissive, pore-forming α subunits are assembled in correct fashion; moreover, small changes in the pore are registered with great sensitivity via measurement of block parameters. Thus, CTX has been used to locate the ion conduction pore (MacKinnon and Miller, 1989), to estimate α subunit stoichiometry (MacKinnon, 1991), to assess the shape of the external pore vestibule (Goldstein et al., 1994; Ranganathan et al., 1996), to confirm the structural quality of purified channel complexes (Doyle et al., 1998), and to count intact channels on cell surfaces (Sun et al., 1994; Aggarwal and MacKinnon, 1996). Second, channels formed by HM-Kv*-Kv* subunits must recapitulate those formed by monomer subunits with good fidelity. Previous work has shown that linking voltage-gated K+ channel α subunits in pairs leads to assembly of channels that gate and conduct like their native counterparts while higher-order complexes sometimes act anomalously (Liman et al., 1992; Yang et al., 1997; Tu and Deutsch, 1999). Thus, K_{ATP} channels formed naturally by four pore-forming $K_{IR}6.2$ subunits and four SUR1 accessory subunits are well mimicked by expression of linked SUR1-$K_{IR}6.2$ subunits (even though SUR1 has 1581 residues and 12 transmembrane spans), and SUR1-$K_{IR}6.2$-$K_{IR}6.2$ subunits expressed with SUR1 monomers form 4:4 SUR1/$K_{IR}6.2$ channels (Clement et al., 1997). Here, we observed channels formed by HM + Kv* or HM-Kv*-Kv* subunits to operate alike and confirmed that each linked subunit contributed to function and/or pore formation. Finally, our conclusions assume that HM and Kv* serve as faithful surrogates for MinK and KCNQ1 despite changes required to allow antibody binding and high-affinity CTX blockade, a notion supported by the similar biophysical attributes of the resultant channels.

MinK Valence Judged by Subunit Mixing Has Been Confusing
In the past, we judged it 20 times more likely that two MinK subunits were in each I_{Ks} channel rather than four, based on suppression of current when wild-type MinK was mixed with an inhibitory MinK mutant (Wang and Goldstein, 1995); it was argued that both MinK types were incorporated into I_{Ks} channels in unbiased fashion, as they enjoyed equivalent surface expression and it appeared that a single mutant MinK ablated channel function. We suspect other mixing studies have offered higher estimates for MinK number due to differential

subunit expression, nondominant phenotype, and nature of I_{Ks} channel gating. Thus, despite a $\sim$140-fold change in CTX affinity for Kv* channels with M or HM subunits (Table 1), we could not assess subunit valence by study of altered CTX block upon subunit mixing, as done with Shaker channel α subunits (MacKinnon, 1991), because steady-state surface levels of M were higher than HM (not shown). Assessing changes in I_{Ks} gating can be problematic because the currents do not saturate (e.g., reach equilibrium) so that thermodynamic assumptions that allow determination of classical gating parameters are not met and values reported for I_{Ks} are, perforce, experiment dependent. Thus, we found activation of HM + Kv*, HM-Kv*-Kv*, and HM-Kv* channels to be nearly equivalent in voltage dependence (see Results) and kinetics (time to half-maximal current, $T_{1/2} = 1.47 \pm 0.07$ s, 1.38 ± 0.07 s, and 1.48 ± 0.05 s, respectively, 5 s pulses to 20 mV, n = 10–13) and readily distinguishable from Kv* channels ($T_{1/2} = 0.043 \pm 0.003$ s, n = 10–13). Wang and colleagues (1998) similarly found M + KCNQ1 channels to have the same voltage dependence and activation kinetics as M-KCNQ1-KCNQ1 and M-KCNQ1 channels and I_{Ks} currents in neonatal mouse ventricular myocytes but argued for variable MinK valence because they found M-KCNQ1 activation to slow on M coexpression (from $T_{1/2} = \sim 1.05$ to 1.3 s at 40 mV, 2 s pulses). In contrast, we found no evidence for incorporation of additional MinK subunits either using the sensitive assay of CTX block kinetics (Table 1) or in studies of activation kinetics ($T_{1/2}$) by expression of HM with HM-Kv*-Kv*, HM with HM-Kv*, or M with M-Kv* (n = 12–16).

Trajectory of MinK in I_{Ks} Channels
The location of MinK relative to KCNQ1 in I_{Ks} channels is another subject of debate (Wang et al., 1998; Kurokawa et al., 2001). We have argued that MinK residues gain exposure in the outer pore vestibule (Wang et al., 1996), travel close to the ion conduction pathway near the selectivity filter (Tai and Goldstein, 1998; Chen et al., 2003), and influence the structure of the inner pore vestibule from an unknown distance (Sesti et al., 2000). Here, M and HM were found to significantly alter CTX affinity for the channels formed with Kv* in opposing manner (Table 1). This is not, however, new evidence that MinK is in the pore. Changes in CTX block could result from through-space electrostatic effects or altered pore structure due to effects on other portions of the protein. Indeed, we suspect HM enhanced CTX on rate via electrostatic attraction because HM carries a net charge of -7 e relative to M in a region known to affect I_{Ks} pore function, and CTX on rate is sensitive to charge on the toxin ($+5$ e at neutral pH) and channel (MacKinnon and Miller, 1989; Goldstein and Miller, 1991; Goldstein et al., 1994; Wang et al., 1996; Chen et al., 2003). The -25 mV shift in activation $V_{1/2}$ for HM + Kv* compared to M + Kv* channels may have a similar basis. Indeed, neither M nor HM altered affinity of the small pore blocker TEA for channels with Kv*, as shown with M and KCNQ1-K318I, V319Y subunits (Kurokawa et al., 2001), although M did alter TEA block of channels with wild-type KCNQ1 (Goldstein and Miller, 1991).

Future Issues

One unexplored puzzle is how channels of HM-Kv* subunits fold. Both antibody binding studies (Figure 5) and toxin blocking studies (Table 1) indicate that all four HM subunits gain exposure on the cell surface. Thus, forced transition from two to four HM (HM-Kv*-Kv* versus HM-Kv*) increased toxin on rate by a factor of 2. Conversely, the destabilizing effect of MinK on bound CTX (enhancing off rate) was the same with two or four MinK subunits in each channel (M-Kv*-Kv* versus M-Kv*, Table 1). This suggests that third and fourth MinK domains are distant from the pore if they are on the surface (although perhaps close enough that a third and fourth HM can act in through-space fashion to speed toxin binding). A related issue is whether transgenic mice expressing a linked gene for human M-KCNQ1 channels with 4:4 valence (Chiello Tracy et al., 2003) show different effects than they would with I_{ks} channels of natural 2:4 composition.

No prior studies have suggested that I_{ks} channels have fewer than two MinK subunits. Indeed, our mixing study suggested that incorporation of one MinK subunit was ~100 times less likely than two MinK subunits (Wang and Goldstein, 1995). While this report argues directly for 2:4 valence by two new strategies, we have thus far been unable to use these approaches to rule out one MinK per channel because linked subunits with 1:4 stoichiometry (i.e., HM-Kv*-Kv*-Kv*-Kv*) have given very small currents of variable character.

Correct 4:4 subunit assembly of SUR1 + $K_{IR}6.2$ subunits is demanded for release from endoplasmic reticulum and surface expression of K_{ATP} channels (Zerangue et al., 1999). Similarly, soluble cytoplasmic Kvβ subunits assemble with Kv1 and Kv4 K⁺ channel α subunits with 4:4 stoichiometry (Trimmer, 1998). How then can biosynthesis of I_{ks} channels be rationalized? Evidence that K⁺ channels assemble as dimers of α subunit dimers (Tu and Deutsch, 1999) suggests I_{ks} channels may form by aggregation of KCNQ1 dimers and MinK monomers to form trimers with subsequent coupling of two MinK/α subunit trimers.

MiRP subunits enjoy broad tissue distribution, and the number of recognized native K⁺ channels that appear to require these β subunits to achieve normal function is increasing rapidly. As I_{ks} channels formed in oocytes and COS7 cells contain two MinK and four pore-forming KCNQ1 subunits, it seems reasonable to expect the same arrangement will apply when I_{ks} channels assemble in native cells and that other channels incorporating MiRPs will employ the same valence. The list of published, purported MiRP/α subunit partnerships now includes (*KCNE1*) MinK with KCNQ1 or HERG; (*KCNE2*) MiRP1 with HERG, KCNQ1, Kv4.2, Kv4.3, or HCN1; (*KCNE3*) MiRP2 with Kv3.4, KCNQ1, or HERG; xMiRP2 (from *X. laevis*) (Anantharam et al., 2003) with HERG; (*KCNE4*) MiRP3 with KCNQ1; (*KCNE5*) MiRP4 with KCNQ1; and MPS-1 + KVS-1 (a MiRP and α subunit in *C. elegans*) (Bianchi et al., 2003).

Experimental Procedures

Full descriptions can be found online at http://www.neuron.org/cgi/content/full/40/1/15/DC1.

Molecular Biology

Human KCNQ1 and MinK were in a dual-purpose vector for cRNA production or CMV-based expression. In HM, MinK residues 1–43 are replaced with hMiRP1 residues 1–49 carrying an epitope (YPYD-VPDYA) between 30 and 31. Creation of linked subunits is described online at http://www.neuron.org/cgi/content/full/40/1/15/DC1.

Electrophysiology

Xenopus oocytes injected with cRNA (5 ng pore-former, 1 ng M or HM) were studied by two-electrode voltage clamp with constant perfusion (~1 ml/min, exchange < 3 s) at room temperature, as before (Chen et al., 2003). Data were sampled at 1 kHz and filtered at 0.25 kHz. Raw currents are in figure legends; for data analysis, leak correction was performed offline to assess only slowly activating currents. G-V curves fitted to a Boltzman, $G/G_{max} = (1 + e^{[(V-V_{0.5})/V_s]})^{-1}$, to give $V_{0.5}$ and V_s.

Standard bath solution was (in mM) 96 NaCl, 2 KCl, 1 MgCl₂, 1.8 CaCl₂, 5 HEPES/NaOH (pH 7.5). Recombinant CTX was freshly diluted from 100 μM stock just prior to use. Bovine serum albumin (BSA) was present at 1 mg/ml in CTX solutions. TEA•Cl was used without osmotic compensation. KCl was altered by isotonic exchange for NaCl. TEA was used to reveal contaminating currents from channels with xKCNQ1, as Kv* is sensitive but endogenous xKCNQ1 (with M or HM) is not (Ki > 100 mM, not shown).

Protocols
Blockade, 5 s test pulse to 20 mV from −90 mV every 10 or 15 s. Reversal potential, 5 s at 40 mV from −90 mV with test tail pulse from −120 mV to 40 mV or −160 mV to 0 mV. Activation, 5 s at −80 mV to 80 mV (10 mV steps) with tail pulse at −70 mV.

CTX Blockade

Unblocked fractional current at equilibrium fitted to Equation 7 gives the K_i. Block proceeds via scheme in Equation 1, so K_{on} is a second-order association rate constant and K_{off} a first-order dissociation rate constant. With a single bound state and rapid addition and removal of toxin compared to kinetics of block and unblock (Miller et al., 1985; MacKinnon and Miller, 1988; Goldstein and Miller, 1993), the time constant for approach to equilibrium with a CTX concentration [CTX] is

$$\tau_{on} = 1/(K_{on} \times [CTX] + K_{off}); \qquad (3)$$

the time constant for relaxation to unblocked current level on CTX removal is

$$\tau_{off} = 1/K_{off}; \qquad (4)$$

unblocked fractional current at equilibrium (f_u) is related to K_{on} and K_{off} as

$$f_u = K_{off}/(K_{on} \times [CTX] + K_{off}); \qquad (5)$$

the equilibrium inhibition constant for half-maximal blockade is

$$K_i = K_{off}/K_{on}; \qquad (6)$$

and the dose dependence for block described by

$$f_u = (1 + ([CTX]/K_i)^h)^{-1}, \qquad (7)$$

where h is a coefficient. CTX block parameters are thus multiply determined by measurement of toxin association and dissociation.

CTX Synthesis and Binding Assay

Radioactive CTX synthesis and binding were as described (Sun et al., 1994). Binding, COS7 cells (culture conditions online at http://www.neuron.org/cgi/content/full/40/1/15/DC1) suspended in PBS and diluted to an OD₆₀₀ of 0.2 (~2.9 × 10⁵ cells/ml) were used in 250 μl duplicate or triplicate aliquots for control (to assess nonspecific ³H-CTX binding with excess nonradioactive CTX, 4 μM) and test samples (to assess total binding); specific was total (test) less nonspecific (control) counts. ³H-CTX (34 nM) was applied in PBS with 1 mg/ml of BSA for 30 min. All steps at 4°C. Toxin released during washes was the same (±5%) for all channels. Average signal-to-noise ratio was 2.

Anti-HA Antibody Binding Assay of HM

Surface levels of subunits on COS7 cells were assessed as for oocytes (Zerangue et al., 1999; O'Kelly et al., 2002) and yeast cells (Sesti et al., 2003). Briefly, live cells were blocked with PBS-containing goat serum, stained with rat monoclonal anti-HA antibody and then a peroxidase-conjugated secondary goat anti-rat IgG1 antibody prior to assessment in a luminometer. Average signal-to-noise ratio was 5.

References

Abbott, G.W., and Goldstein, S.A.N. (1998). A superfamily of small potassium channel subunits: form and function of the MinK-related peptides (MiRPs). Q. Rev. Biophys. *31*, 357–398.

Abbott, G.W., and Goldstein, S.A. (2002). Disease-associated mutations in *KCNE* potassium channel subunits (MiRPs) reveal promiscuous disruption of multiple currents and conservation of mechanism. FASEB J. *16*, 390–400.

Aggarwal, S.K., and MacKinnon, R. (1996). Contribution of the S4 segment to gating charge in the Shaker K$^+$ channel. Neuron *16*, 1169–1177.

Anantharam, A., Lewis, A., Panaghie, G., Gordon, E., McCrossan, Z.A., Lerner, D.J., and Abbott, G.W. (2003). RNA interference reveals that endogenous *Xenopus* MinK-related peptides govern mammalian K$^+$ channel function in oocyte expression studies. J. Biol. Chem. *278*, 11739–11745.

Barhanin, J., Lesage, F., Guillemare, E., Fink, M., Lazdunski, M., and Romey, G. (1996). KvLQT1 and IsK (minK) proteins associate to form the I$_{Ks}$ cardiac potassium current. Nature *384*, 78–80.

Bianchi, L., Kwok, S.M., Driscoll, M., and Sesti, F. (2003). A potassium channel-MiRP complex controls neurosensory function in *Caenorhabditis elegans*. J. Biol. Chem. *278*, 12415–12424.

Chen, H., Sesti, F., and Goldstein, S.A.N. (2003). Pore and state-dependent cadmium block of I$_{Ks}$ channels formed with MinK-55C and wild type KCNQ1 subunits. Biophys. J. *84*, 3679–3689.

Chiello Tracy, C., Cabo, C., Coromilas, J., Kurokawa, J., Kass, R.S., and Wit, A.L. (2003). Electrophysiological consequences of human I$_{Ks}$ channel expression in adult murine heart. Am. J. Physiol. Heart Circ. Physiol. *284*, H168–H175.

Clement, J.P., 4th, Kunjilwar, K., Gonzalez, G., Schwanstecher, M., Panten, U., Aguilar-Bryan, L., and Bryan, J. (1997). Association and stoichiometry of K$_{ATP}$ channel subunits. Neuron *18*, 827–838.

Doyle, D.A., Morais Cabral, J., Pfuetzner, R.A., Kuo, A., Gulbis, J.M., Cohen, S.L., Chait, B.T., and MacKinnon, R. (1998). The structure of the potassium channel: molecular basis of K$^+$ conduction and selectivity. Science *280*, 69–77.

Goldstein, S.A., and Miller, C. (1991). Site-specific mutations in a minimal voltage-dependent K$^+$ channel alter ion selectivity and open-channel block. Neuron *7*, 403–408.

Goldstein, S.A., and Miller, C. (1992). A point mutation in a Shaker K$^+$ channel changes its charybdotoxin binding site from low to high affinity. Biophys. J. *62*, 5–7.

Goldstein, S.A., and Miller, C. (1993). Mechanism of charybdotoxin block of a voltage-gated K$^+$ channel. Biophys. J. *65*, 1613–1619.

Goldstein, S.A., Pheasant, D.J., and Miller, C. (1994). The charybdotoxin receptor of a Shaker K$^+$ channel: peptide and channel residues mediating molecular recognition. Neuron *12*, 1377–1388.

Gross, A., Abramson, T., and MacKinnon, R. (1994). Transfer of the scorpion toxin receptor to an insensitive potassium channel. Neuron *13*, 961–966.

Kavanaugh, M.P., Hurst, R.S., Yakel, J., Varnum, M.D., Adelman, J.P., and North, R.A. (1992). Multiple subunits of a voltage-dependent potassium channel contribute to the binding site for tetraethylammonium. Neuron *8*, 493–497.

Kurokawa, J., Motoike, H.K., and Kass, R.S. (2001). TEA$^+$-sensitive KCNQ1 constructs reveal pore-independent access to KCNE1 in assembled I$_{Ks}$ channels. J. Gen. Physiol. *117*, 43–52.

Liman, E.R., Tytgat, J., and Hess, P. (1992). Subunit stoichiometry of a mammalian K$^+$ channel determined by construction of multimeric cDNAs. Neuron *9*, 861–871.

MacKinnon, R. (1991). Determination of the subunit stoichiometry of a voltage-activated potassium channel. Nature *350*, 232–235.

MacKinnon, R., and Miller, C. (1988). Mechanism of charybdotoxin block of the high-conductance, Ca^{2+}-activated K$^+$ channel. J. Gen. Physiol. *91*, 335–349.

MacKinnon, R., and Miller, C. (1989). Mutant potassium channels with altered binding of charybdotoxin, a pore-blocking peptide inhibitor. Science *245*, 1382–1385.

Miller, C., Moczydlowski, E., Latorre, R., and Phillips, M. (1985). Charybdotoxin, a protein inhibitor of single Ca^{2+}-activated K$^+$ channels from mammalian skeletal muscle. Nature *313*, 316–318.

O'Kelly, I., Butler, M.H., Zilberberg, N., and Goldstein, S.A. (2002). Forward transport. 14-3-3 binding overcomes retention in endoplasmic reticulum by dibasic signals. Cell *111*, 577–588.

Ranganathan, R., Lewis, J.H., and MacKinnon, R. (1996). Spatial localization of the K$^+$ channel selectivity filter by mutant cycle-based structure analysis. Neuron *16*, 131–139.

Sanguinetti, M.C., Curran, M.E., Zou, A., Shen, J., Spector, P.S., Atkinson, D.L., and Keating, M.T. (1996). Coassembly of KvLQT1 and Mink (Isk) proteins to form cardiac I$_{Ks}$ potassium channel. Nature *384*, 80–83.

Schulze-Bahr, E., Wang, Q., Wedekind, H., Haverkamp, W., Chen, Q., and Sun, Y. (1997). *KCNE1* mutations cause Jervell and Lange-Nielsen syndrome. Nat. Genet. *17*, 267–268.

Seebohm, G., Scherer, C.R., Busch, A.E., and Lerche, C. (2001). Identification of specific pore residues mediating KCNQ1 inactivation. A novel mechanism for long QT syndrome. J. Biol. Chem. *276*, 13600–13605.

Sesti, F., and Goldstein, S.A.N. (1998). Single-channel characteristics of wildtype I$_{Ks}$ channels and channels formed with two minK mutants that cause long QT syndrome. J. Gen. Physiol. *112*, 651–664.

Sesti, F., Tai, K.K., and Goldstein, S.A.N. (2000). MinK endows the I$_{Ks}$ potassium channel with sensitivity to internal TEA. Biophys. J. *79*, 1369–1378.

Sesti, F., Rajan, S., Gonzalez-Colaso, R., Nikolaeva, N., and Goldstein, S.A.N. (2003). Hyperpolarization moves S4 sensors inward to open MVP, a methanococcal voltage-gated potassium channel. Nat. Neurosci. *6*, 353–361.

Splawski, I., Tristani-Firouzi, M., Lehmann, M.H., Sanguinetti, M.C., and Keating, M.T. (1997). Mutations in the hminK gene cause long QT syndrome and suppress I$_{Ks}$ function. Nat. Genet. *17*, 338–340.

Sun, T., Naini, A.A., and Miller, C. (1994). High-level expression and functional reconstitution of Shaker K$^+$ channels. Biochemistry *33*, 9992–9999.

Tai, K.K., and Goldstein, S.A.N. (1998). The conduction pore of a cardiac potassium channel. Nature *391*, 605–608.

Trimmer, J.S. (1998). Regulation of ion channel expression by cytoplasmic subunits. Curr. Opin. Neurobiol. *8*, 370–374.

Tu, L., and Deutsch, C. (1999). Evidence for dimerization of dimers in K$^+$ channel assembly. Biophys. J. *76*, 2004–2017.

Tzounopoulos, T., Guy, H.R., Durell, S., Adelman, J.P., and Maylie, J. (1995). minK channels form by assembly of at least 14 subunits. Proc. Natl. Acad. Sci. USA *92*, 9593–9597.

Wang, K.W., and Goldstein, S.A.N. (1995). Subunit composition of minK potassium channels. Neuron *14*, 1303–1309.

Wang, K.-W., Tai, K.-K., and Goldstein, S.A.N. (1996). MinK residues line a potassium channel pore. Neuron *16*, 571–577.

Wang, W., Xia, J., and Kass, R.S. (1998). MinK-KvLQT1 fusion proteins, evidence for multiple stoichiometries of the assembled IsK channel. J. Biol. Chem. *273*, 34069–34074.

Yang, Y., Yan, Y., and Sigworth, F.J. (1997). How does the W434F mutation block current in Shaker potassium channels? J. Gen. Physiol. *109*, 779–789.

Zerangue, N., Schwappach, B., Jan, Y.N., and Jan, L.Y. (1999). A new ER trafficking signal regulates the subunit stoichiometry of plasma membrane K_{ATP} channels. Neuron *22*, 537–548.